Rewetting of three drained peatlands drives congruent compositional changes in pro- and eukaryotic microbiomes through environmental filtering

Micha Weil[1], Haitao Wang[1], Mia Bengtsson[1], Anke Günther[2], Gerald Jurasinski[2], John Couwenberg[3], Wakene Negassa[2], Dominik Zak[4, 5], Tim Urich[1*]

[1] Institute of Microbiology, University of Greifswald, Felix-Hausdorff-Str. 8, 17487 Greifswald, Germany

[2] Faculty of Agriculture and Environmental Sciences, University of Rostock, Justus-von-Liebig-Weg 6, 18059 Rostock, Germany

[3] Institute of Botany and Landscape Ecology, University of Greifswald, Soldmannstraße 15, 17487 Greifswald, Germany, partner of the Greifswald Mire Center

[4] Department of Chemical Analytics and Biogeochemistry, Leibniz-Institute of Freshwater Biology and Inland Fisheries, Müggelseedamm 301, 12587 Berlin, Germany

[5] current address: Department of Bioscience, Aarhus University, Vejlsøvej 25, 8600 Silkeborg, Denmark

*corresponding author, Institute of Microbiology, University of Greifswald, Felix-Hausdorff-Str. 8, 17487 Greifswald, Germany; Tel.: +49 (0)3834 420 5904; E-Mail: tim.urich@uni-greifswald.de

Running Title: Changes in peatland microbiome through rewetting

Summary

Drained peatlands are significant sources of the greenhouse gas (GHG) carbon dioxide. Rewetting is a proven strategy to protect the large carbon stocks; however, it can also lead to increased emissions of the potent GHG methane. The response to rewetting of soil microbiomes as drivers of these processes is poorly understood, as are the biotic and abiotic factors that control community composition.

We analyzed the soil microbiomes of three contrasting pairs of minerotrophic fens subject to decade-long drainage and subsequent rewetting. Analyses comprised qPCR of methanogens, amplicon sequencing of prokaryotic and eukaryotic rRNA genes, and abiotic soil properties including moisture and dissolved organic matter.

The composition of pro- and eukaryotic communities was fen-type-specific, but all rewetted site showed higher abundance of anaerobic taxa. Based on multi-variate statistics and network analyses we identified soil moisture as major driver of community composition. Furthermore, salinity drove the separation between coastal and freshwater fen communities. Methanogens were more than tenfold more abundant in rewetted than in drained sites while their abundance was lowest in the coastal fen, likely due to competition with sulfate reducers. These results shed light on the factors that structure fen microbiomes via environmental filtering.

1. Introduction

Peatlands cover 3% of the global land surface and contain about 30% of the global soil organic carbon (SOC) pool in the form of peat (Joosten *et al.*, 2016). During the agricultural industrialization in the 20th century, many temperate mires in Europe but also other parts of the world were drained to be used as grassland or arable farming. Globally, drained or generally disturbed peatlands cover 0.3% of the global land surface but contribute approx. 5% of all anthropogenic greenhouse gas (GHG) emissions including carbon dioxide (CO_2), methane (CH_4) and nitrous oxide (N_2O). The latter holds also for Germany, where drained peatlands cover approx. 5 % of the surface (Freibauer *et al.*, 2009; Joosten and Couwenberg, 2009). In the German federal state of Mecklenburg-West-Pomerania, peatlands cover 13% of the land surface, their large majority being drained (approx. 90%) and emitting about 30% of the total GHG budget in the region (Ziebarth *et al.*, 2009; Greifswald Mire Center, 2019).

Peat accumulates under water-logged conditions, when more plant biomass is formed by growth than is mineralized by the prokaryotic and eukaryotic soil (micro-)biome. Water is a key factor, limiting decomposition by cutting off the supply of oxygen and other alternative terminal electron acceptors (TEA) to mineralizing microbiota (Dean *et al.*, 2018). Under anoxic conditions plant litter accumulates and forms peat with a high content of soil organic matter that accumulates over millennia. Changes in ecology and hydrology of peatlands can lead to substantial changes in GHG fluxes by changing the peatland biogeochemistry (Parish *et al.*, 2008). If peatlands are drained, formerly anoxic soil layers become aerated and carbon is released as CO_2 during aerobic mineralization by peat microbiota (Conrad, 1996).

In the past three decades, several 100 000 ha of European peatlands were rewetted for environmental protection and to recover some of their ecological functions (Andersen *et al.*, 2013; Chimner *et al.*, 2017). Rewetting is a proven strategy to protect the large SOC stocks; however, it can also lead to increased emissions of the potent GHG CH_4 and to the release of dissolved organic matter (DOM). While effects of peatland rewetting on GHG and DOM fluxes are comparably well studied (Couwenberg *et al.*, 2011; Hahn *et al.*, 2015; Estop-Aragonés *et al.*, 2016; Wilson, D. Blain, D. Cowenberg, J. Evans,

63 C.D. Murdiyarso, D. Page, S. E. Renou-Wilson, F. Rieley, J.O. Sirin, A. Strack. M. Tuittila, 2016; Lyu *et al.*,
64 2018), the impact on the peat microbiota, who is the primary driver of GHG production and thus
65 emissions is poorly understood, because it has been not well studied in temperate fens (see an
66 exception in (Wen *et al.*, 2018). The major players in soil organic matter (SOM) decomposition in peat
67 soils are microorganisms of the bacterial, archaeal and eukaryotic (e.g. fungi) domains of life,
68 participating in a cascade of SOM degradation steps (Andersen *et al.*, 2013; Yarwood, 2018), eventually
69 resulting in emissions of CH_4 and CO_2. Hydrolytic extracellular enzymes catalyze the initial
70 decomposition of polymeric SOM. Under anoxic conditions, this step has been considered as a major
71 bottleneck and the one determining the rate of downstream processes (Conrad, 1996). Further steps
72 in the degradation are carried out through anaerobic respiratory microorganisms (like denitrifiers, iron
73 reducers and sulfate reducers), fermentative and methanogenic microorganisms (Dean *et al.*, 2018),
74 while methanotrophic microorganisms constitute the biological filter for CH_4 emissions from peat (e.g.
75 Tveit et al., 2013). Remarkably, many novel players in soil CH_4 cycling have been identified in the past
76 few years (Söllinger *et al.*, 2016; Welte *et al.*, 2016; Sorokin *et al.*, 2017; Singleton *et al.*, 2018). Thus,
77 despite more than half a century of research on methanogens, their diversity, physiology and
78 interactions within the microbiom are still poorly understood.

79 It is crucial to obtain a mechanistic understanding of microbial responses and dynamics upon rewetting
80 to suggest robust managing practices for climate-optimal peatland protection and utilization (e.g.
81 paludiculture, Joosten et al., 2016). Environmental filtering, i.e. the selection of certain taxa through
82 abiotic environmental conditions, is considered to be a major mechanism structuring communities
83 (Cadotte and Tucker, 2017). In this context, identifying the main environmental drivers of both total
84 microbiome composition, as well as the abundance of relevant functional groups involved in carbon
85 cycling and methanogenesis is essential.

86 In this study we explore the effect of rewetting on temperate fen prokaryotic and eukaryotic microbial
87 communities. For this purpose, three pairs of drained (dry; terms in parenthesis are used in the
88 following to refer to these ecosystems and their states) and rewetted (wet) fens with contrasting water

89 tables and vegetation were investigated: a brackish coastal fen (Coast), a percolation fen (Perco) and
90 an alder carr (Alder). We hypothesize that despite the obvious structural and geo genetic differences,
91 congruent effects of rewetting will be detectable in the microbiomes of the three peatland types
92 because of environmental filtering. Possible controlling factors of community composition, like DOM
93 quantity and quality, soil moisture, soil/water salinity, were also determined to allow for analyzing the
94 effect of rewetting on key players of SOM mineralization and CH_4-cycling microorganisms.

95 A suite of cultivation-independent microbiological and geochemical methods was applied, including
96 DOM profiling as well as qPCR of the methanogenesis key enzyme *mcrA* and 16S and 18S rRNA gene
97 amplicon based microbiome analysis. Our results may contribute to better understand how
98 microbiomes respond to rewetting and to the relevant controlling environmental factors. Microbiome-
99 based proxies for predicting CH_4 emissions from rewetted peatlands eventually derive.

100 2. Results

101 **Study site and their soil properties**

102 Our investigations took place in three pairs of drained and rewetted peatlands (see table 1 and
103 materials and methods for details).

104 Table 1: Sampling site characteristics

Abbreviation	Site	State (year of rewetting)	Water table	Peat thickness	Dominant plant species
Alder	Alder carr	dry	-100 cm	60 cm	Black Alder (*Alnus glutinosa),* Ground Elder (*Aegopodium podagraria*) and Common Nettle (*Urtica dioica*)
		wet (1999)	+15 cm	> 1 m	Black Alder (*Alnus glutinosa), Greater Pond Sedge (Carex riparia)*
Coast	Coastal fen	dry	-70 cm	70 cm	Creeping Bentgrass (*Agrostis stolonifera*)
		wet (1993)	-5 cm	30 cm	Creeping Bentgrass (*Agrostis stolonifera*)
Perco	Percolation fen	dry	-20 cm	6 m	Creeping Buttercup (*Ranunculus repens*), Tufted Hairgrass (*Deschampsia cespitosa*)
		wet (1998)	+10 cm	6 m	Lesser Pond Sedge (*Carex acutiformis*)

105

In general, the gravimetric water content was higher in the rewetted than in the drained sites (Table S1). However, there was only a minor difference between $Perco_{dry}$ (74.2% ± 5.1) and $Perco_{wet}$ (75.4% ± 5.3), because of a high water-table near the soil surface in $Perco_{dry}$ at the time of sampling. In all of the drained sites and in $Coast_{wet}$, the water content increased with depth. In $Perco_{wet}$ and $Alder_{wet}$ (78.7 ± 4.6) with water table 10 cm above ground, the water content increased slightly with depth or did not change. The lower gravimetric water contents in $Coast_{dry}$ (45.9% ± 6.7), $Coast_{wet}$ (53.8% ± 10.03), and $Alder_{dry}$ (46.3% ± 7.0) corresponded with higher amounts of mineral soil compounds.

The sampling sites were generally acidic; pH values varied between fen types but increased with depth in all drained sites. Lower pH values were detected in $Coast_{dry}$ (3.9 - 4.0) and $Alder_{dry}$ (4.2 - 4.7), while pH values were higher in $Perco_{dry}$ (5.0-5.2) and $Coast_{wet}$ (4.7 - 6.1). In $Alder_{wet}$ (5.1 - 5.1) and $Perco_{wet}$ (5.4 – 5.4), the pH values did not change with depth (Table S1).

Salinity in the freshwater fens was generally low (0.08 - 0.49‰). The influence of the nearby brackish bay water with a salinity of 8‰ led to a higher salinity in $Coast_{dry}$ (1.32‰) and in $Coast_{wet}$ (5.2‰) (Table S1).

DOM concentrations in the soil extracts of $Alder_{wet}$ and $Coast_{wet}$ were higher than in the drained sites. In $Perco_{wet}$ DOM values measured near the surface were higher than in $Perco_{dry}$, but they showed a strong decrease with increasing depth. The distribution of separate DOM fractions, i.e. biopolymers, humic or humic-like substances and low molecular organic matter (lCOM) followed the overall pattern of total DOM (Table S1).

Total carbon (TC) and total nitrogen (TN) content of peat decreased with depth in $Alder_{dry}$, $Coast_{dry}$ and $Coast_{wet}$. In contrast, TC increased with depth in $Alder_{wet}$, $Perco_{dry}$ and $Perco_{wet}$. In $Alder_{wet}$, $Perco_{wet}$ and $Perco_{dry}$ TN did not change with depth. Total sulfur (TS) content increased with depth in $Alder_{dry}$, $Alder_{wet}$ and $Perco_{wet}$ while it decreased with depth in $Coast_{dry}$ and $Coast_{wet}$. In $Perco_{dry}$, no change was observed over depth (Table S1).

131 **Diversity of prokaryotes and eukaryotes**

132 Alpha diversity of prokaryotes, calculated from 16S rRNA gene amplicon sequence variants (ASVs), was
133 significantly higher in the two freshwater peatlands than in the coastal fen (Fig. S1, $p < 0.001$). Alpha
134 diversity was slightly higher in rewetted than in drained sites, but this was significant only in the coastal
135 fen ($p < 0.001$). Alpha diversity showed a positive correlation with soil water content, TC, TN and DNA
136 content (Fig. S2).

137 Similarly, alpha diversity of eukaryotes in freshwater peatlands was higher than in the coastal fen
138 ($p = 0.11$). In contrast to prokaryotes, eukaryote alpha diversity was significantly lower in rewetted
139 sites than in drained sites in Perco ($p = 0.015$), while no significant difference was observed in Alder
140 and Coast. Alpha diversity of eukaryotes decreased with depth in the rewetted sites. For both pro- and
141 eukaryotes, alpha diversity was negatively correlated with salinity (Fig. S2).

142

143 **Microbiota composition**

144 Community composition in 16S rRNA and 18S rRNA sequencing analysis of prokaryotes and eukaryotes
145 showed remarkably similar patterns in the non-metric multidimensional scaling (NMDS) plot (Fig. 1),
146 with a significant clustering of microbiota from the same sampling sites (PERMANOVA $p = 0.001$). While
147 the communities of freshwater fens Alder and Perco showed some overlap, the microbiota in Coast
148 were clearly separated along NMDS axis 1, possibly driven by the differences in abiotic factors, such as
149 salinity, total nitrogen (TN), total carbon (TC), C/N ratio and DOM compounds (Fig. 1). Nevertheless,
150 the pro- and eukaryotic microbiota of the dry and wet sites of each fen type were consistently
151 separated along NMDS axis 2, indicating that the water table of the sites influenced the community
152 composition (PERMANOVA $p = 0.001$, $R^2 = 0.267$). Depth showed less impact on community
153 composition (PERMANOVA $p = 0.161$, $R^2 = 0.046$), although some clustering according to sample depth
154 was observed.

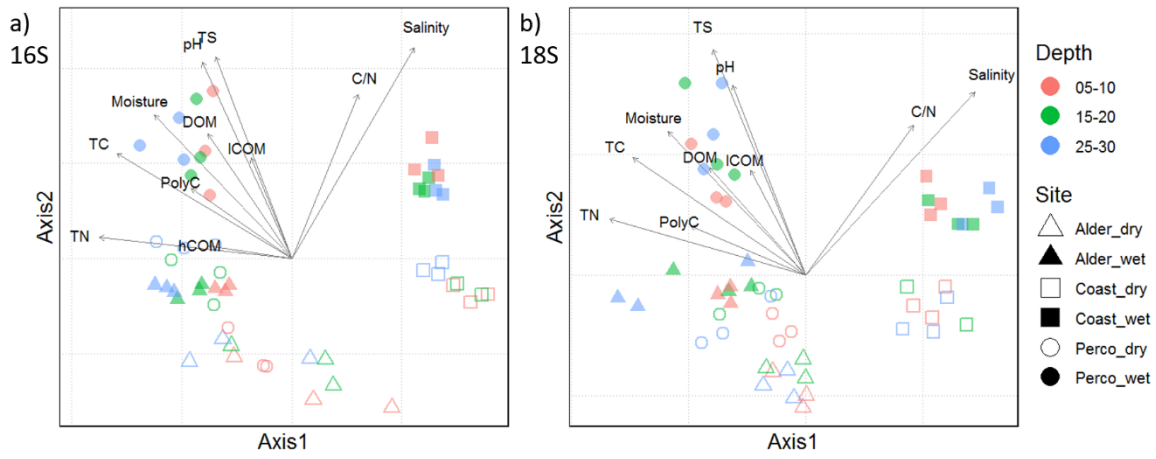

Figure 1: NMDS plots showing (a) prokaryotic and (b) eukaryotic community compositions. Symbols show triplicates of cores and indicate the study sites; the color indicates the depth in cm (see legend). Environmental vectors with a significance of $p < 0.05$ are shown in black. TN: total nitrogen, hCOM: humic like carbon, TC: total carbon, PolyC: Carbon polymers, DOM: dissolved organic matter, lCOM: low molecular organic matter, TS: total Sulphur, C/N: carbon/nitrogen ratio.

Pro- and eukaryotic community compositions were compared between fen types, water conditions (dry/wet) and sampling depths (Fig. 2a). We detected a higher relative abundance of Acidobacteria in drained sites, while Betaproteobacteria, Deltaproteobacteria (mainly comprised of Myxobacteria and sulfate reducers) and Bathyarchaeota showed higher values in all rewetted sites and $Perco_{dry}$. SPAM and Latescibacteria were not detected in Coast, but they occurred in the freshwater fens, whereas Actinobacteria showed higher values in Coast than in Alder and Perco.

The eukaryotic community varied considerably between fen types and water condition (Fig. 2b). Among the fungi, ASVs of Ascomycota (which contain saprophytes, yeasts and several plant pathogens) showed high relative abundance in each site, except $Perco_{dry}$. ASV values of Basidiomycota decreased with depth in Alder and Coast, and showed higher relative abundance in these two site than in Perco. ASV values of Glomerycota, which form arbuscular mycorrhiza with plants, comprising mostly Mortirellales were high in $Alder_{dry}$ and $Perco_{dry}$.

174 Among the protists, ASV values of Apicomplexa were high (up to 40%) in $Perco_{dry}$, but accounted for
175 less than 5% in other sites. Cercozoa, which contain micro-predators among other life styles, had
176 higher values in the freshwater sites Alder and Perco. Relative abundance of Lobosa and Ciliophora,
177 also potential micro-predators, was high in $Alder_{wet}$ and in sites with high water content (rewetted
178 sites and $Perco_{dry}$) respectively.

179 Among the Metazoa, Nematoda showed highest relative abundance, followed by Arthropoda. The
180 latter accounted for 5-10% of total amplicons in Coast and $Perco_{dry}$ and the 5-10 cm layer of $Alder_{dry}$,
181 while their values were lower in $Alder_{wet}$ and $Perco_{wet}$.

182

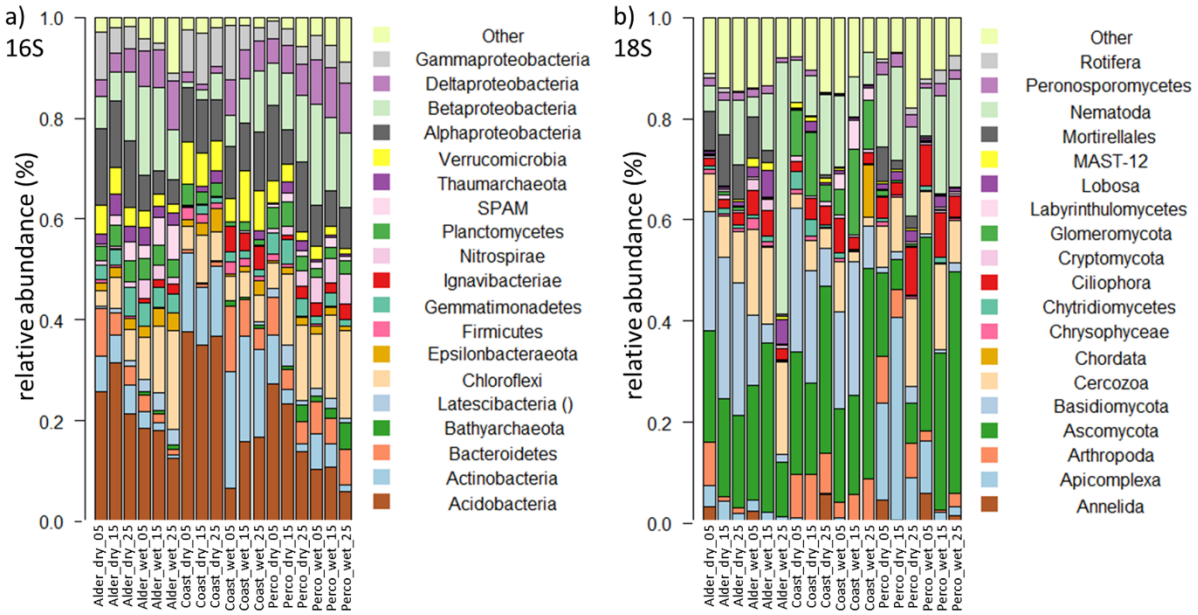

183

184 Figure 2: Composition of prokaryotic and eukaryotic microbial communities of drained and rewetted
185 fens. a) Taxonomic composition of prokaryotic 16S rRNA genes displayed on phylum level, with
186 Proteobacteria shown on class level. b) Taxonomic composition of eukaryotic 18S rRNA genes, on
187 phylum level. Bars show triplicate of cores; phyla with < 1% abundance are displayed as "other". The
188 sample ID on x-axis displays fen type and depth in cm.

189

190 A co-occurrence network was constructed to explore the potential interactions between pro- and
191 eukaryotic species. The network shows two distinct clusters of ASVs (Fig. 3). Color coding of the vertices
192 according to association with sites shows that ASVs within the same site were more connected than
193 different sites (Fig. 3b). However, ASVs associated with rewetted sites shows little connections with
194 those from the drained sites (Fig. 3c), highlighting the significant effect of water conditions on the co-
195 occurrence patterns. Similarly, the indicator taxa from Coast were mostly connected with each other,
196 and indicator taxa from Perco and Alder were also distinctly connected in the network (Fig. 3b).
197 However, there were quite some shared indicator taxa from both Perco and Alder, indicating
198 similarities between these two habitats compared with Coast, which we already detected in
199 community composition (Figs. 1 and 2). The degree and closeness centrality of the indicator taxa were
200 higher in the wet sites than in the dry sites (Fig. 3c). particularly in Coast, followed by Alder, and Perco
201 (Fig. 3b, c). The transitivity was higher among Coast indicators compared with those from Alder.

202 The prokaryotic indicator taxa in drained sites mainly comprised ASVs from Acidobacteria and Alpha-
203 and Gamma-Proteobacteria, whereas the main indicator taxa of rewetted sites were Beta- and Delta-
204 Proteobacteria. Beta- and Delta-Proteobacteria were also the main phyla in both hydrological status
205 (Fig. 2). Plants (Tracheophyta) accounted for the largest proportion of the eukaryotic indicator taxa for
206 both water condition and site. Nematoda ASVs accounted for a larger proportion in the drained than
207 in the rewetted sites; Ascomycota showed the reverse trend.

208 In the network with only connections between eukaryotes and prokaryotes (Fig. 3a), eukaryotes
209 showed higher degrees of connection compared with prokaryotes (Fig. 3). Among the eukaryotes,
210 fungi (Ascomycota, Basidiomycota and Glomeromycota) possessed the most connections with the
211 prokaryotes.

212

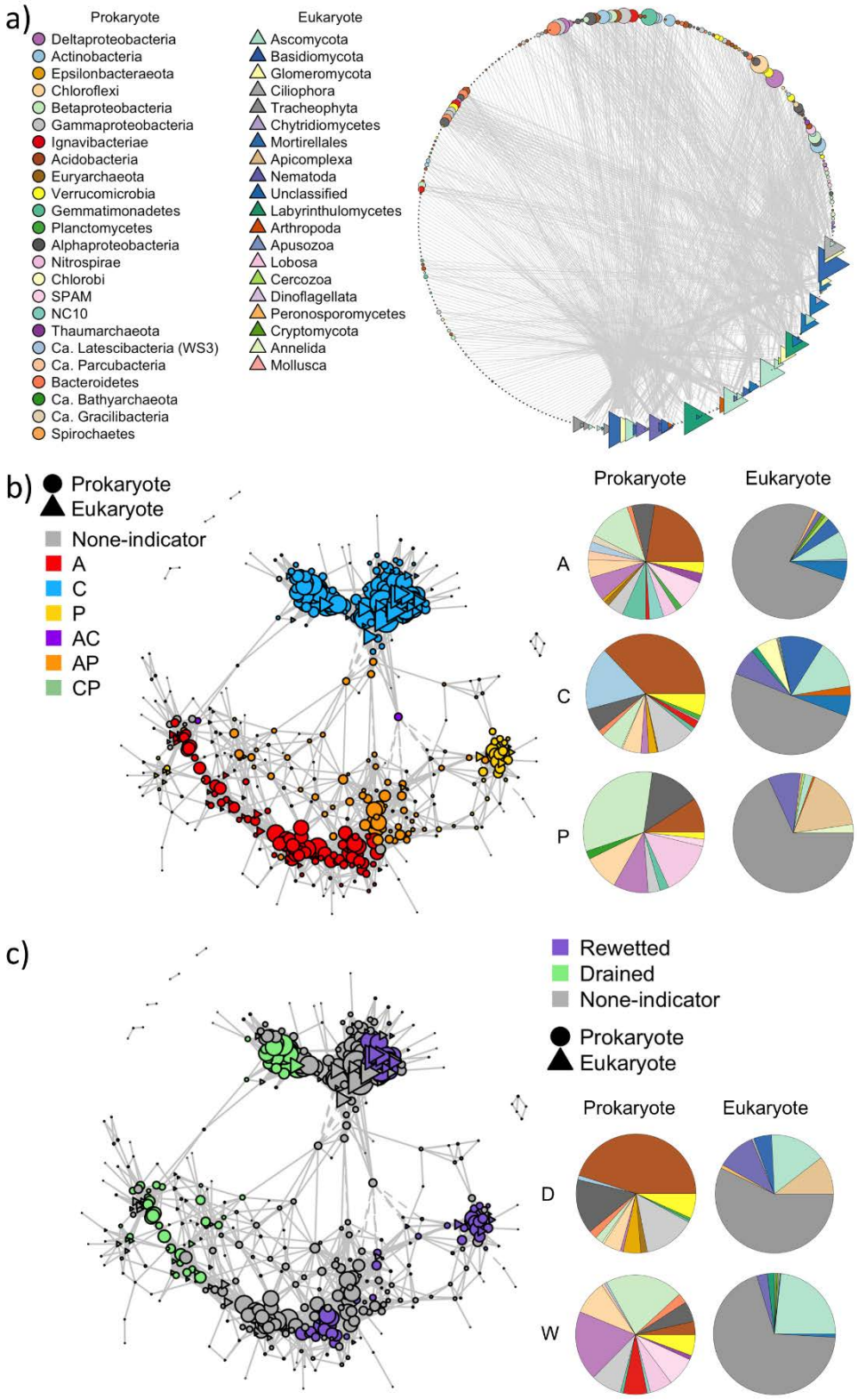

Figure 3: Co-occurrence networks. a) Co-occurrence network of prokaryotes and eukaryotes corresponding to the indicator ASVs of 16S and 18S rRNA amplicon sequencing. ASVs with relative abundances lower than 0.05% were discarded. b) Co-occurrence network of ASVs associated with (A)

217 alder carr, (C) coastal fen and (P) percolation fen. c) Co-occurrence of ASVs associated with drained (D)
218 and rewetted (W) sites. ASVs were associated with sites using the *indicspecies* package (De Cáceres
219 and Legendre, 2009).. Solid lines indicate significant positive Spearman's rank correlations
220 ($r > 0.7$. $p < 0.01$) between prokaryotic and eukaryotic Indicator ASVs, dashed lines indicate significant
221 negative correlations ($r < -0.7$. $p < 0.01$). Nodes are sized according to the number of correlating
222 neighbors (degree) and color-coded according to site type or water condition (drained/rewetted). The
223 relative abundance of prokaryotes and eukaryotes associated with the different site types is shown on
224 the right hand side of b) and c).

225

226 **Methanogens**

227 The abundance of methanogens in the samples, assessed by quantitative polymerase chain reaction
228 (qPCR) of the *mcrA* gene, ranged from 2.1×10^5 to 5.1×10^7 gene copies g^{-1} dry soil (Fig. 4). The *mcrA*
229 gene abundance was significantly higher in the three rewetted sites compared with the drained sites
230 (Kruskal-Wallis test, $H = 16.5$, $p < 0.001$). The difference was largest in the top soils, where *mcrA*
231 abundances were much higher in rewetted sites. In $Alder_{wet}$ methanogen abundance decreased
232 significantly with depth, while it was rather constant in $Perco_{wet}$. In contrast, methanogen abundance
233 in $Alder_{dry}$ was rather constant or increased with depth ($Coast_{dry}$ and $Perco_{dry}$). Positive correlations
234 were observed between *mcrA* abundance and water, DNA and DOM content (strongest with
235 biopolymers and lCOM; Fig. S2). Furthermore, TC and TN as well as pH value were positively correlated
236 with *mcrA* abundance (Fig. S2).

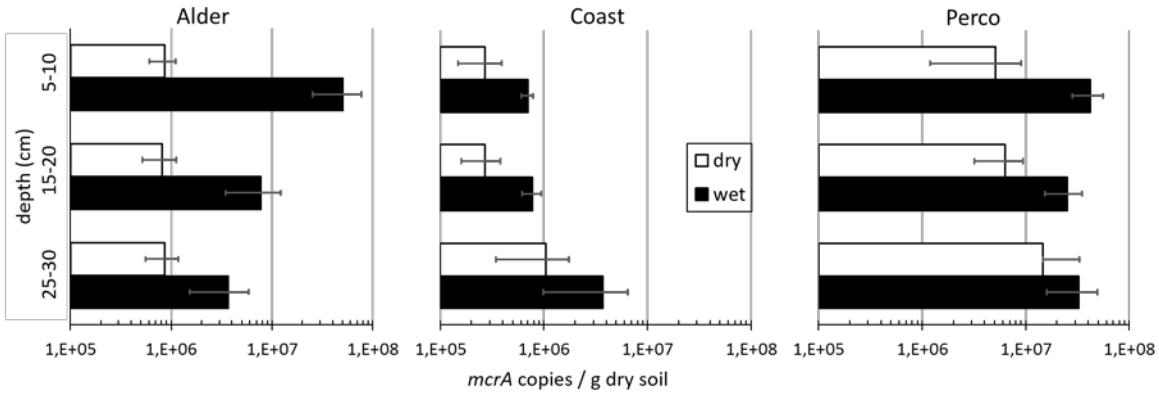

Figure 4: Abundance of methanogens. *mcrA* gene copy numbers per gram dry soil based on qPCR. X-axis shows mcrA copies per g dry soil, drained sites in white, rewetted sites in black bars, error bars show standard deviation of triplicate soil cores.

The relative abundance of methanogens in the prokaryotic microbiota was low. Methanogen-affiliated ASVs in the amplicon sequence datasets were on average below 0.25% of total 16S rRNA amplicons (Fig. 5). In most of the drained fens, methanogen ASVs were even absent, although they were detectable by *mcrA* qPCR (see above, Fig. 4). Upper soil samples of $Alder_{wet}$ and $Coast_{wet}$ showed highest abundances, while methanogens were more abundant in the lower samples of $Perco_{wet}$. Methanobacteriales and Methanosarcinales (including the families Methanosaetaceae and Methanosarcinaceae) were the dominant orders in $Alder_{wet}$ and $Coast_{wet}$, while methanogens were more diverse in $Perco_{wet}$, where Methanomassiliicoccales and Methanomicrobiales were also present.

Despite apparently missing out on some methanogens in the amplicon data, the relative abundance calculated from *mcrA* gene copies per g dry soil (qPCR) shows a clear positive correlation with the relative abundance of methanogenic archaea in 16S rRNA amplicon (Spearman correlation, R= 0.578; $p < 0.001$).

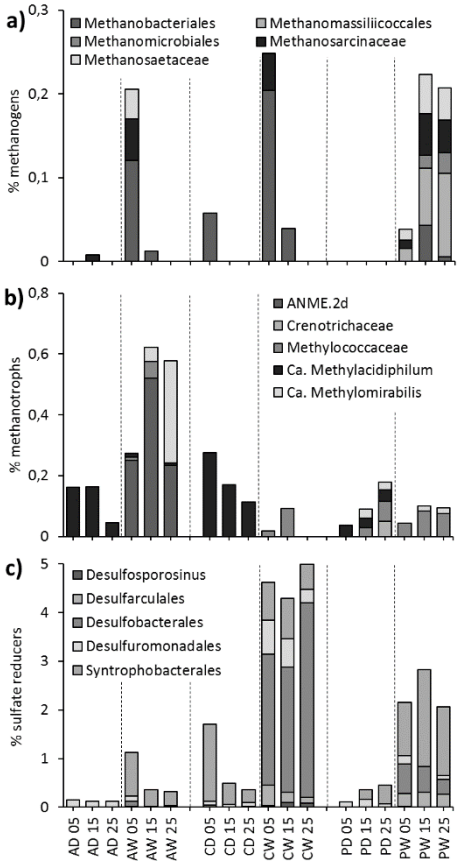

Figure 5: Relative abundance of functional groups in 16S rRNA gene amplicon datasets. a) Methanogens, b) methanotrophic bacteria and archaea, c) sulfate reducers. Barplots show relative abundance. X-axes represent fen type: alder carr (A), coastal fen (C), percolation fen (P), hydrological state drained (D) and rewetted (W), depth in cm (05, 15, 25). Data are shown as mean values of triplicate soil cores.

Methanotrophs

16S rRNA genes of known methanotrophic prokaryotes were found in all sites (Fig. 5b), but never exceeded 1% of all prokaryotic 16S rRNA genes on average. Their relative abundance and taxon composition differed both between fen types and dry/wet. In drained fens ASVs affiliated with *Ca.* Methylacidiphilum (phylum Verrucomicrobia) were dominant across the soil profile. In contrast, ASVs of Methylococcaceae (class Gammaproteobacteria) were the most abundant methanotrophs in $Coast_{wet}$ and $Perco_{wet}$. Putative anaerobic methanotrophs affiliated with *Ca.* Methanoperedens

268 (ANME-2d, archaea) and with *Ca*. Methylomirabilis (NC10 phylum), were the dominant methanotroph
269 guild at the $Alder_{wet}$ site.

270 **Sulfate reducers**

271 ASVs of known sulfate reducers were generally more abundant than methanogens and methanotrophs
272 (between 0.1% and 5% on average, Fig. 5c). Like methanogens, their relative abundance was higher in
273 rewetted sites than in drained sites. Highest relative abundance was observed in the $Coast_{wet}$, which is
274 exposed to recurrent influx of sea water. ASVs of Desulfobacterales were particularly abundant in this
275 site. Desulfarculales and Desulfosporosinus were only detected in rewetted sites, while
276 Desulfuromonadales occurred in all sites. Relative abundance of sulfate reducers was positively
277 correlated to salinity, but not to total sulfur (Fig. S2).

278

279 3. Discussion

280 To our knowledge, this is the first comprehensive study investigating the impact of long-term rewetting
281 (>> 10 years) on freshwater and coastal fen microbiomes. The parallel study of three different fen
282 types allowed for the identification of overarching factors next to fen type-specific factors. The NMDS
283 plots of both prokaryotes and eukaryotes were almost superimposable. It is remarkable that rewetting
284 caused highly congruent effects on beta-diversity of all three domains of life and it is conceivable that
285 water table and salinity were the main environmental filters among the physicochemical controlling
286 factors. Rewetting resulted in more anoxic conditions in the rewetted sites compared with the drained
287 sites. Increased anoxia is supported by several lines of evidence, including (1) a higher moisture
288 content and (2) higher proportions of presumably fermentative microorganisms and (3) higher
289 proportion of taxa with different types of anaerobic respiration, such as methanogenesis and sulfate
290 reduction.

291 **Environmental filtering effect on pro- and eukaryotic community composition**

292 The network analysis confirmed the conclusions we drew from the community composition: there are
293 more taxa indicative for each of the different fen types than for water status. Consequently, site
294 location has a more significant effect on the community assemblages. The higher degree and closeness
295 centrality of indicators in rewetted sites indicates more connections in these sites. This might be due
296 to that higher water flow rates in soils create greater homogeneity, and hence weak niche
297 differentiation, contributing to stronger interactions between soil microbes. Further, it might reflect
298 the close metabolic interactions in anaerobic microbiomes during plant biomass degradation (Schink,
299 1997; Tveit *et al.*, 2015). Main taxa of indicator ASVs in rewetted sites were Chloroflexi and Delta- and
300 Betaproteobacteria, which contained ASVs known from anoxic environments, also highly abundant in
301 the wet communities (Fig. 2 and Fig. 3) (He *et al.*, 2015). In the drained sites, most indicator taxa were
302 from Acidobacteria, the predominant phylum, which would correspond with the general acidic site
303 conditions. Drainage and subsequent oxidation processes in peat soils are associated with acid
304 production and depending on the buffer capacity of soils pH may go down by one or two units
305 compared with pre-drained conditions (Lamers, 1998). In contrast, rewetting with base-rich water will
306 increase alkalinity and pH (Cusell *et al.*, 2013). Especially the two dominant classes Acidobacteria
307 (subdivision 1) and Solibacteres (subdivision 3) decreased in relative abundance upon rewetting
308 (Supplementary Fig. S4), which is in line with the obligatory aerobic lifestyle of most characterized
309 member species (Eichorst *et al.*, 2018). Members of the aerobic Acidobacteria play important roles in
310 carbohydrate degradation, but some subdivisions also contain facultative or obligate anaerobic species
311 (Eichorst *et al.*, 2018; Hausmann *et al.*, 2018). Other putative anaerobic phyla such as Ignavibacter and
312 Bathyarchaeota occurred only in rewetted sites and deep layers of drained sites. Obviously, soil
313 moisture acted as environmental filter leading to community compositional changes from oxygen-
314 dependent taxa (drained) to anaerobic and fermentative taxa in the rewetted peat soils (Fig. S3). A
315 second likely environmental filter in our study is salinity. The higher connectivity and transitivity of
316 indicators from Coast may result from environmental filtering through higher salinity in these sites,
317 leading to a change in microbial community with increases of Actinobacteria and sulfate reducers and
318 decrease of methanogens (Dang et al., 2018, and see below).

319 Remarkably, the largest proportion of eukaryotic indicator ASVs originated from Tracheophyta
320 (plants), indicating that the interaction between plants and the soil microbiota is very important.
321 Similar to the prokaryotes, the interaction was even stronger in rewetted sites than in drained sites. In
322 Coast with the lowest moisture content, Tracheophyta ASVs showed lower values than in Perco and
323 Alder. Among the animals, Nematoda indicator ASVs accounted for a larger proportion in drained sites,
324 likely because they are dependent on oxic conditions.

325 In the network, we also observed that eukaryotes had higher degrees than prokaryotes. The
326 prokaryotes mostly connected with fungi, like Ascomycota, Basidiomycota and Glomeromycota,
327 suggesting that especially fungi may drive the composition of prokaryotic communities. We found
328 fewer eukaryotic than prokaryotic ASVs, suggesting that one eukaryote was probably connected with
329 multiple prokaryotes, as implied by higher degrees of connection for eukaryotes. Similarly, the richness
330 of eukaryotes was far less than the richness of prokaryotes, which is common for soil microbiota, as
331 shown before in e.g. Tveit et al. (2015). Therefore, our results potentially suggest this as a universal
332 rule of pro-eukaryote interactions.

333

334 **The influence of rewetting on methanogens**

335 The important group of methanogenic archaea was hardly included in the analysis of microbial
336 networks and played no role in the determination of indicator taxa. The reason was the low relative
337 abundance of methanogens in the amplicon datasets of the microbiota, being less than three per mil
338 in all samples. Although their relative abundance in the microbiota was low even under rewetted
339 conditions, their abundance per gram soil was high, especially in the rewetted sites. Wet peatlands are
340 known to contribute a large share of the global CH_4 emissions (Nazaries *et al.*, 2013; Joosten *et al.*,
341 2016). The higher *mcrA* abundance after rewetting (Fig. 4) could lead to increased CH_4 emissions from
342 peatlands, as is the case in rice paddy fields (Reim *et al.*, 2017; Wen *et al.*, 2018). Interestingly, their
343 abundance was high in the rewetted top soils, at least in $Alder_{wet}$ and $Perco_{wet}$, and not in the subsoils.

344 This is in contrast to general assumptions about their vertical distribution in the soil profile (reviewed
345 in Dean et al., 2018) and corroborates recent findings from other ecosystems (Hahn-Schöfl *et al.*, 2011;
346 Angle *et al.*, 2017). This observation makes peatland management practices such as top soil removal
347 attractive for mitigation of CH_4 emissions from peatlands (Harpenslager *et al.*, 2015; Zak *et al.*, 2018;
348 A.Guenther, unpublished). The abundance of methanogens was strongly correlated with soil water
349 content (Fig. S2), which drives anoxia in the soil. However, many other factors like substrate availability
350 of DOM, especially lCOM, C and N content of soil, degradation status of the peat and sulfate and nitrate
351 concentration all correlated with methanogen abundance per gram dry soil as well (Fig. S2). One
352 significant factor was salinity, resulting from brackish water intrusions from the Baltic Sea in $Coast_{wet}$,
353 which led to large differences between freshwater fens (Alder and Perco) and Coast. In $Coast_{wet}$ the
354 abundance of methanogens per gram soil was at least 10x lower than in the freshwater sites $Alder_{wet}$
355 and $Perco_{wet}$. Thus, this environmental filtering through salinity likely leads to lower CH_4 emissions,
356 also shown before in several studies(Neubauer *et al.*, 2013; He *et al.*, 2015; van Dijk *et al.*, 2017).

357 The strong positive correlation of *mcrA* gene abundance in qPCR with the relative abundance of
358 methanogenic archaea in 16S rRNA gene amplicon datasets proves the validity of the measured results.
359 However, in most of the drained peats ($Perco_{dry}$, most $Alder_{dry}$ and $Coast_{dry}$), methanogenic taxa were
360 not present in the dataset, although *mcrA* genes were quantified by qPCR. This can be explained by
361 the rather shallow average sequencing depth of 20,000 reads per sample, giving a taxon detection limit
362 of about 0.05‰ in the microbiota, and thus taxa with lower abundances could not be detected. Still,
363 the distribution of methanogenic taxa led to the assumption that substrate availability was different
364 in the sites. While hydrogenotrophic Methanobacteriales were dominant in $Coast_{wet}$, $Coast_{dry}$ and
365 $Alder_{wet}$, $Perco_{wet}$ showed a high variability in methanogenic groups. Here the Methanosarcinales
366 families of Methanosaetaceae (obligate acetoclastic) and Methanosarcinaceae (flexible substrate
367 spectrum) occurred, as did the Methanomicrobiales and the Methanomassiliicoccales (that use the H_2
368 dependent methylotrophic pathway). Methanomassiliicoccales were detected in every site with
369 Methanomassiliicoccales specific qPCR primers AS1/AS2 (Mihajlovski *et al.*, 2010) (data not shown).

370 Their high abundance in $Perco_{wet}$ indicates that besides the well reported hydrogenotrophic and
371 acetotrophic pathways (Lyu *et al.*, 2018), methylotrophic methanogenesis may contribute more to
372 peatland CH_4 emissions than currently assumed (Söllinger *et al.*, 2016; Zalman *et al.*, 2017).

373

374 **Interactions between methanogens, methanotrophs and sulfate reducers**

375 The second important player in peatland CH_4 emissions is the heterogenic group of methanotrophic
376 Bacteria and Archaea, acting as biological CH_4 filter through aerobic or anaerobic oxidation of the
377 produced CH_4 (reviewed in Nazaries et al., 2013 and Knief, 2015). Do the methanogens influence
378 abundance of methanotrophs? The methanotrophic groups differed with site, and were generally
379 lower abundant in the drained sites where *Ca.* Methylacidiphilum aerobic CH_4 oxidizers were
380 dominant. These organisms were originally isolated from acidic and volcanic environments, but have
381 recently also been found in pH neutral environments (van Teeseling *et al.*, 2014; Vaksmaa *et al.*, 2016).
382 They are characterized by growth on low CH_4 concentrations, and are possibly atmospheric CH_4
383 oxidizers, which would make them independent of substrate supply by methanogens. As found in
384 other wetland studies (e.g. Tveit et al., 2013, Smith et al., 2018) aerobic CH_4 oxidizers of
385 Methylococcaceae dominated in the wet sites. The anaerobic group *Ca.* Methylomirabilis (Vaksmaa *et*
386 *al.*, 2016), which uses oxygen from nitrite to reduce CH_4 appeared in the sites with highest water
387 content ($Alder_{wet}$, $Perco_{dry}$ and $Perco_{wet}$). The anaerobic CH_4 oxidizing ANME-2d (*Ca.*
388 Methanoperedens) which reduce CH_4 by the reverse methanogenic pathway (Welte *et al.*, 2016) were
389 detected in the water-covered fen $Alder_{wet}$. Although we did not find a clear correlation between
390 methanogen and methanotroph abundance (see Wen *et al.*, 2018 for similar findings), we did find a
391 strong division of anaerobic and aerobic methanotrophs depending on water content and therefore
392 oxygen availability, between sites and depths.

393 What is the basis of the environmental filter leading to the low methanogen abundance in the coastal
394 fen? It is known that sulfate reducers can have an impact on methanogens, because methanogens and

395 sulfate reducers not only share the anaerobic niche, but also compete for the same substrates, such
396 as hydrogen (Kristjansson and Schönheit, 1983; Thauer *et al.*, 2008; He *et al.*, 2015) and acetate
397 (Kristjansson *et al.*, 1982). Due to their higher substrate affinity, sulfate reducers can outcompete
398 methanogens, leading to lower methanogen abundance in the presence of sulfate reducers
399 (Kristjansson *et al.*, 1982; van Dijk *et al.*, 2017). In fact, Desulfobacterales, known competitors for H_2
400 as a substrate for methanogenesis, occurred in the coastal site $Coast_{wet}$ with a large proportion, which
401 was associated with a more than tenfold lower *mcrA* gene abundance than in $Alder_{wet}$ and $Perco_{wet}$.
402 The influence of salinity in tidal marshes is also known to decrease CH_4 emission compared to
403 freshwater sites (Poffenbarger *et al.*, 2011; van Dijk *et al.*, 2017). Although no CH_4 emissions were
404 measured in this study, the higher methanogen abundance in freshwater peatland suggests higher
405 emission rates (Bartlett *et al.*, 1987) than from the coastal fen. Our study provides microbiome-based
406 insights into the environmental filtering effects of rewetting of fen ecosystems and suggests that, in
407 terms of minimizing CH_4 emissions, increased salinity and/or top soil removal might be promising
408 options. Future analysis of seasonal microbiome dynamics and measurements of CH_4 fluxes will
409 provide evidence, whether these predictions hold true.

410

411 # 4. Experimental procedures

412 **Sites and sampling**

413 All sampling sites, alder carr, coastal fen and percolation fen, are located in north-eastern Germany
414 (Fig. S5). The alder carr is part of the Recknitz river valley, was drained at least from 1786 on and has
415 been used as a managed forest. The sub-site $Alder_{wet}$ (54°13'N 12°49'E) was unintentionally flooded in
416 1999 due to a blocked drain and has remained wet since then. In the sub-site $Alder_{dry}$ (54°13'N 12°51'E)
417 long-term deep drainage $Alder_{dry}$ has caused subsidence of the soil surface of about 1 m.

418 The coastal fen, located on a peninsula, was naturally episodically flooded by brackish seawater coming
419 from the Bay of Greifswald of the Baltic Sea, typically during winter storm surges. The entire area was

420 diked in 1850 to allow for pasture and other agricultural use. In 1993, the dykes around the sub site
421 $Coast_{wet}$ (54°16'N 13°39'E) were removed and, subsequently, the site was episodically flooded again.
422 The sub-site $Coast_{dry}$ (54°16'N 13°39'E) in contrast remains behind the dyke and, thus, cut off from the
423 seawater influence. Both, $Coast_{wet}$ and $Coast_{dry}$ are used as cattle pastures.

424 The percolation fens, representing the third type of peatlands, are located in the catchment areas of
425 the rivers Trebel and Recknitz. Both sites were deeply drained for intensive land-use and used as deep-
426 drained grassland in the 20th century. In 1998, the water table at the sub-site $Perco_{wet}$ (54°10'N 12°74'E)
427 in the Trebel valley was raised again to 5-10 cm above ground level as part of a large rewetting project
428 (EU LIFE project) (Ministerium für Bau, Landesentwicklung und Umwelt, M-V 1998). In contrast, the
429 water table of the still drained sub-site $Perco_{dry}$ (54°13'N 12°63'E) in the Recknitz valley remains several
430 decimeters below the surface and is mown 1-2 times per year.

431 At all sites peat samples were taken as triplicates at 5-10 cm, 15-20 cm and 25-30 cm depths (Fig. S5)
432 using a gouge. The samples were stored in 50-ml reaction tubes on ice over night until further
433 processing.

434 **Soil physico-chemical properties**

435 Soil moisture was measured gravimetrically by drying 2-3 g of soil over night at 90°C until mass
436 constancy. Soil moisture is expressed as the percentage of lost water weight to wet soil weight. The
437 potential soil pH was measured at room temperature with a digital pH meter (pH 540 GLP, WTW,
438 Weilheim, Germany) in 0.01 M $CaCl_2$ solution with a 1: 2.5 soil to solution ratio. Concentrations of total
439 C, N and S were measured using a CNS analyzer (Vario MICRO cube – Elementar Analysensysteme
440 GmbH Langenselbold, Germany). DOM was measured in soil extracts derived from mixing 3 g of
441 previously frozen soil with 30 ml 0.1 M NaCl in 50 ml reaction tubes with subsequent shaking (vortex,
442 180 rpm) for 30 min. Extracts were filtered through 0.45 µm (pore size) sodium acetate filters, which
443 were prewashed with 50 µl deionized H_2O to remove soluble acetate. The concentrations and the
444 composition of DOM based on size categories were determined using a size-exclusion chromatography

445 (SEC) with organic carbon and organic nitrogen detection (LC-OCD-OND analyzer, DOC-Labor Huber,
446 Karlsruhe, Germany) (Huber *et al.*, 2011). The DOM was classified into three major sub-categories: (i)
447 biopolymers, (ii) humic or humic-like substances including building blocks, and (iii) low molecular-
448 weight substances. Time between sample preparation and analysis did never exceed two weeks and
449 samples were stored at 5°C to avoid significant changes of DOM composition (Heinz and Zak, 2018).
450 Soluble reactive phosphorus was determined with the ammonium molybdate spectrometric method
451 (DIN EN 1189 D11) using a Cary 1E Spectrophotometer (Varian). $N\text{-}NH_4^+$ and $N\text{-}NO_3^-$ were determined
452 calorimetrically using the photometry CFA method (Skalar SAN, Skalar Analytical B.V., The
453 Netherlands) according to the guidelines in EN ISO 11732 (DEV-E 23) and EN ISO 13395 (DEV, D 28),
454 respectively.

455 **DNA extraction and PCR/qPCR**

456 DNA was extracted from 0.25 g soil using the DNeasy PowerSoil Kit (QIAGEN, Hilden, Germany)
457 according to the manufacturer´s recommendation. The bead beating step was performed using a
458 FastPrep®-24 5G instrument (MP Biomedicals, Santa Ana, USA), with intensity 5.0 for 45 s. DNA
459 concentrations were measured with Qubit®2.0 dsDNA High Sensitivity and dsDNA Broad Range
460 assays (Thermo Fisher, Waltham, USA). DNA size was analyzed using 1% agarose gels.
461

462 Quantitative polymerase chain reaction was used to measure the abundances of the *mcrA* gene, coding
463 for methyl coenzyme M reductase subunit A. Quantification of *mcrA* gene copies in peat soil DNA
464 extracts was performed on a qTOWER 2.2 (Analytic Jena, Jena, Germany). The primer pair of forward
465 mlas-mod and reverse *mcrA*- rev (Steinberg and Regan, 2009) was used. For each reaction, 15 µl of
466 PCR mixture contained 7.5 µl of innuMIX qPCR MasterMix SyGreen (Analytic Jena, Jena, Germany),
467 0.75 µl of each primer (10 pmol/µl), 5 µl of ddH2O and 1 µl of template DNA. Duplicate measurements
468 of two concentrations (1 and 2 ng/µl) were performed for each DNA sample. Assay condition was 95°C
469 for 5 min, 35 cycles of 95°C for 30 s, 55°C for 45 s and 72°C for 45°C, followed by melting curve analysis.
470 PCR-product specificity was confirmed by melting point analysis. *mcrA* gene copy numbers were

471 calculated from a standard curve obtained by serially diluting a standard from 10^6 to 10^1 *mcrA* gene
472 copies per µl. The standard was created with above-mentioned primers by amplifying *mcrA* genes from
473 cow rumen fluid (Söllinger *et al.*, 2016) and cloning them into the pGEM®-Teasy vector system
474 (Promega, Mannheim, Germany). Amplicons for *mcrA* standard were generated with vector-specific
475 primers sp6 and T7 and the resulting PCR product was cleaned with DNA purification kit (Biozym,
476 Hessisch Oldendorf, Germany), quality-controlled by agarose gel electrophoresis and quantified with
477 Qubit®2.0 dsDNA High Sensitivity assay. The qPCR assay had the following parameters: slope: 3.41-
478 3.52, efficiency: 0.92-0.96, R^2: > 0.995.

479 **Amplicon sequencing and bioinformatics**

480 16S and 18S rRNA gene amplicons were prepared and sequenced using 300 bp paired-end read
481 Illumina MiSeq V3 sequencing by LGC Genomics (Berlin, Germany). This comprised 16S and 18S rRNA
482 gene PCR amplification, Illumina MiSeq library preparation and sequencing using the primer pair 515YF
483 (GTG YCA GCM GCC GCG GTA A)/ B806R (GGA CTA CNV GGG TWT CTA AT) (Walters *et al.*, 2015) for
484 prokaryotes and 1183F (AATTTGACTCAACRCGGG)/ 1443R (GRGCATCACAGACCTG) (Ray *et al.*, 2016)
485 for eukaryotes.

486 The data were processed using R version 3.5.1 (The R Core Team, 2018). 16S rRNA and 18S rRNA gene
487 amplicon sequences were quality filtered, de-replicated and clustered into ASVs using the *dada2*
488 package (Callahan *et al.*, 2016). The chimeric sequences were de-novo checked and removed with
489 *dada2*. Then the representative sequence of each ASV was assigned to taxonomy against a modified
490 version of the SILVA SSUref_NR_128 data base, containing an updated taxonomy for *Archaea* (Lanzén
491 *et al.*, 2012), using the programs BLASTn (Altschul *et al.*, 1990) and Megan 5 (Huson *et al.*, 2016). ASVs
492 that were assigned to Chloroplast or mitochondria were filtered. Due to the low number of sequences
493 (<500) in one sample ($Coast_{dry}$ 2 15) for both 16S and 18S rRNA genes, this sample was discarded from
494 further analysis. After filtering, 1,134,953 and 3,990,919 sequences, sequences were retained and
495 were clustered into 7697 and 5548 ASVs for 16S and 18S rRNA genes, respectively. Plant sequences

496 which accounted for 288 ASVs were filtered for downstream analysis to increase the resolution of
497 other eukaryotic taxa.

498 Alpha diversity (Shannon entropy) of the microbial community was calculated using the package
499 *phyloseq* (McMurdie and Holmes, 2013). ASV count table was then normalized using
500 metagenomeSeq's CSS (cumulative sum scaling) (Paulson *et al.*, 2013). NMDS was performed to
501 analyze the community composition using the package *vegan* (Oksanen *et al.*, 2016) with defaults.
502 Pairwise Spearman's rank correlations were conducted among soil properties, DNA concentrations,
503 qPCR data, NMDS axes and methanogen relative abundances using the package *Hmisc* to detect the
504 significance of the impact of the factors on microbial communities (Harrell and Dunpont, 2019). The
505 soil properties with significant impact were fitted into NMDS ordination using the envfit function in
506 the *vegan* package.

507 The correlations were visualized by heatmap using *corrplot*. All *P*-values for multiple comparisons were
508 adjusted by the false discovery rate (FDR) method and the null hypothesis was rejected when *P*-values
509 were less than 0.05.

510 A co-occurrence network was constructed to explore the potential interactions between species. Plant
511 ASVs were included in network analysis because plant residues are a major part of peat and they might
512 be important in interactions between microbes. To eliminate the influence of rare taxa, ASVs with
513 relative abundances lower than 0.05% were discarded. The pairwise Spearman's rank correlations
514 were conducted with the package Hmisc and all *P*-values were adjusted by the FDR. The cut-offs of
515 adjusted *P*-value and correlation coefficient were 0.01 and 0.7, respectively. The network was
516 visualized using package *igraph* (Csardi, 2019). A network showing the connections between
517 eukaryotes and prokaryotes was sub-selected from the original network by keeping the edges
518 connecting these two groups. The indicators of each group or group combination of a factor (site or
519 water condition) were identified using *indicspecies* package.

The microbial ecological functional groups were predicted using FAPROTAX (Louca *et al.*, 2016), The identified groups were verified based on literature knowledge. ANME2-D group within *Methanosarcina* known as methanotrophic, using the methanogenic pathway in reverse, was excluded from methanogens. All plots were created using package *ggplot2* (Wickham, 2016).

Acknowledgement

The authors would like to thank Florian Beyer for providing the maps and arrangement of figure S5. The European Social Fund (ESF) and the Ministry of Education, Science and Culture of Mecklenburg-Western Pomerania (Germany) funded this work within the scope of the project WETSCAPES (ESF/14-BM-A55-0034/16 and ESF/14-BM-A55-0030/16).

References

Altschul, S.F., W. Gish, W. Miller, E.W. Myers, and D.J. Lipman. 1990. Basic local alignment search tool. J. Mol. Biol. doi: 10.1016/S0022-2836(05)80360-2.

Angle, J.C., T.H. Morin, L.M. Solden, A.B. Narrowe, G.J. Smith, M.A. Borton, C. Rey-Sanchez, R.A. Daly, G. Mirfenderesgi, D.W. Hoyt, W.J. Riley, C.S. Miller, G. Bohrer, and K.C. Wrighton. 2017. Methanogenesis in oxygenated soils is a substantial fraction of wetland methane emissions. Nat. Commun. 8(1): 1567. doi: 10.1038/s41467-017-01753-4.

Bartlett, K.B., D.S. Bartlett, R.C. Harriss, and D.I. Sebacher. 1987. Methane emissions along a salt marsh salinity gradient. Biogeochemistry 4(3): 183–202. doi: 10.1007/BF02187365.

Callahan, B.J., P.J. McMurdie, M.J. Rosen, A.W. Han, A.J.A. Johnson, and S.P. Holmes. 2016. DADA2: High-resolution sample inference from Illumina amplicon data. Nat. Methods 13(7): 581–583. doi: 10.1038/nmeth.3869.

Conrad, R. 1996. Soil Microorganisms as Controllers of Atmospheric Trace Gases (H 2 , CO , CH 4 , OCS , N 2 O , and NO). 60(4): 609–640.

Couwenberg, J., A. Thiele, F. Tanneberger, J. Augustin, S. Bärisch, D. Dubovik, N. Liashchynskaya, D. Michaelis, M. Minke, A. Skuratovich, and H. Joosten. 2011. Assessing greenhouse gas emissions from peatlands using vegetation as a proxy. Hydrobiologia 674(1): 67–89. doi: 10.1007/s10750-011-0729-x.

Dang, C., E.M. Morrissey, W. Virginia, S.C. Neubauer, and R.B. Franklin. 2018. Novel microbial community composition and carbon biogeochemistry emerge over time following saltwater intrusion in wetlands. (July). doi: 10.1111/gcb.14486.

Eichorst, S.A., D. Trojan, S. Roux, C. Herbold, T. Rattei, and D. Woebken. 2018. Genomic insights into the Acidobacteria reveal strategies for their success in terrestrial environments. Environ. Microbiol. 20(3): 1041–1063. doi: 10.1111/1462-2920.14043.

Estop-Aragonés, C., K. Zajac, and C. Blodau. 2016. Effects of extreme experimental drought and rewetting on CO_2 and CH_4 exchange in mesocosms of 14 European peatlands with different nitrogen and sulfur deposition. Glob. Chang. Biol. 22(6): 2285–2300. doi: 10.1111/gcb.13228.

Hahn, J., S. Köhler, S. Glatzel, and G. Jurasinski. 2015. Methane exchange in a coastal fen in the first year after flooding - A systems shift. PLoS One 10(10). doi: 10.1371/journal.pone.0140657.

Hausmann, B., C. Pelikan, C.W. Herbold, S. Köstlbacher, M. Albertsen, S.A. Eichorst, T. Glavina Del Rio, M. Huemer, P.H. Nielsen, T. Rattei, U. Stingl, S.G. Tringe, D. Trojan, C. Wentrup, D. Woebken, M. Pester, and A. Loy. 2018. Peatland Acidobacteria with a dissimilatory sulfur metabolism. ISME J.: 1–14. doi: 10.1038/s41396-018-0077-1.

He, S., S. a Malfatti, J.W. Mcfarland, F.E. Anderson, A. Pati, M. Huntemann, J. Tremblay, T. Glavina, M.P. Waldrop, L. Windham-myers, and G. Tringe. 2015. Patterns in Wetland Microbial Community Composition and Functional Gene Repertoire Associated with Methane Emissions. Mbio.Asm.Org 6(3): 1–15. doi: 10.1128/mBio.00066-15.Editor.

Heinz, M., and D. Zak. 2018. Storage effects on quantity and composition of dissolved organic carbon and nitrogen of lake water, leaf leachate and peat soil water. Water Res. 130: 98–104. doi: 10.1016/j.watres.2017.11.053.

Huber, S.A., A. Balz, M. Abert, and W. Pronk. 2011. Characterisation of aquatic humic and non-humic matter with size-exclusion chromatography - organic carbon detection - organic nitrogen detection (LC-OCD-OND). Water Res. 45(2): 879–885. doi: 10.1016/j.watres.2010.09.023.

Huson, D.H., S. Beier, I. Flade, A. Górska, M. El-Hadidi, S. Mitra, H.J. Ruscheweyh, and R. Tappu. 2016. MEGAN Community Edition - Interactive Exploration and Analysis of Large-Scale Microbiome Sequencing Data. PLoS Comput. Biol. 12(6): 1–12. doi: 10.1371/journal.pcbi.1004957.

Joosten, H., and J. Couwenberg. 2009. Are emission reductions from peatlands measurable, reportable and verifiable? Wetlands: 14. www.wetlands.org.

Joosten, H., A. Sirin, J. Couwenberg, J. Laine, and P. Smith. 2016. The role of peatlands in climate regulation. Peatl. Restor. Ecosyst. Serv. Sci. Policy Pract. (May): 63–76. doi: 10.1017/CBO9781139177788.005.

Knief, C. 2015. Diversity and habitat preferences of cultivated and uncultivated aerobic methanotrophic bacteria evaluated based on pmoA as molecular marker. Front. Microbiol. 6(DEC). doi: 10.3389/fmicb.2015.01346.

589 Kristjansson, J.K., and P. Schönheit. 1983. Why do sulfate-reducing bacteria outcompete
590 methanogenic bacteria for substrates? Oecologia 60(2): 264–266. doi:
591 10.1007/BF00379530.

592 Lanzén, A., S.L. Jørgensen, D.H. Huson, M. Gorfer, S.H. Grindhaug, I. Jonassen, L. Øvreås, and
593 T. Urich. 2012. CREST - Classification Resources for Environmental Sequence Tags. PLoS
594 One 7(11). doi: 10.1371/journal.pone.0049334.

595 Louca, S., L. Wegener Parfrey, and M. Doebeli. 2016. Decoupling function and taxonomy in
596 the global ocean microbiome. Science 353(6305): 1272–1277. doi:
597 10.1126/science.aaf4507.

598 Lyu, Z., N. Shao, T. Akinyemi, and W.B. Whitman. 2018. Current Biology. (Figure 1): 727–732.
599 doi: 10.1016/j.cub.2018.05.021.

600 Mihajlovski, A., J. Doré, F. Levenez, M. Alric, and J.F. Brugère. 2010. Molecular evaluation of
601 the human gut methanogenic archaeal microbiota reveals an age-associated increase of
602 the diversity. Environ. Microbiol. Rep. 2(2): 272–280. doi: 10.1111/j.1758-
603 2229.2009.00116.x.

604 Nazaries, L., J.C. Murrell, P. Millard, L. Baggs, and B.K. Singh. 2013. Methane, microbes and
605 models: Fundamental understanding of the soil methane cycle for future predictions.
606 Environ. Microbiol. 15(9): 2395–2417. doi: 10.1111/1462-2920.12149.

607 Neubauer, S.C., R.B. Franklin, and D.J. Berrier. 2013. Saltwater intrusion into tidal freshwater
608 marshes alters the biogeochemical processing of organic carbon. Biogeosciences
609 10(12): 8171–8183. doi: 10.5194/bg-10-8171-2013.

610 Parish, F., A. Sirin, D. Charman, H. Joosten, T. Minayeva, M. Silvius, and L. Stringer. 2008.

611 Assessment on Peatlands, Biodiversity and Climate Change: Main Report.

612 Paulson, J.N., O. Colin Stine, H.C. Bravo, and M. Pop. 2013. Differential abundance analysis
613 for microbial marker-gene surveys. Nat. Methods. doi: 10.1038/nmeth.2658.

614 Poffenbarger, H.J., B.A. Needelman, and J.P. Megonigal. 2011. Salinity influence on methane
615 emissions from tidal marshes. Wetlands 31(5): 831–842. doi: 10.1007/s13157-011-
616 0197-0.

617 Ray, J.L., J. Althammer, K.S. Skaar, P. Simonelli, A. Larsen, D. Stoecker, A. Sazhin, U.Z. Ijaz, C.
618 Quince, J.C. Nejstgaard, M. Frischer, G. Pohnert, and C. Troedsson. 2016.
619 Metabarcoding and metabolome analyses of copepod grazing reveal feeding preference
620 and linkage to metabolite classes in dynamic microbial plankton communities. Mol.
621 Ecol. 25(21): 5585–5602. doi: 10.1111/mec.13844.

622 Reim, A., M. Hernández, M. Klose, A. Chidthaisong, M. Yuttitham, and R. Conrad. 2017.
623 Response of methanogenic microbial communities to desiccation stress in flooded and
624 rain-fed paddy soil from Thailand. Front. Microbiol. 8(MAY): 1–17. doi:
625 10.3389/fmicb.2017.00785.

626 Schink, B. 1997. Energetics of syntrophic cooperation in methanogenic degradation.
627 Microbiol. Mol. Biol. Rev. 61(2): 262–80.
628 http://www.ncbi.nlm.nih.gov/pubmed/9184013.

629 Singleton, C., C. McCalley, B. Woodcroft, J. Boyd, P. Evans, S. Hodgkins, J. Chanton, S.
630 Frolking, P. Crill, S. Saleska, V. Rich, and G. Tyson. 2018. Methanotrophy across a natural
631 permafrost thaw environment. ISME J. 1. doi: 10.1038/s41396-018-0065-5.

632 Söllinger, A., C. Schwab, T. Weinmaier, A. Loy, A.T. Tveit, C. Schleper, and T. Urich. 2016.

633 Phylogenetic and genomic analysis of Methanomassiliicoccales in wetlands and animal
634 intestinal tracts reveals clade-specific habitat. FEMS Microbiol. Ecol. 92(1): 1–12. doi:
635 10.1093/femsec/fiv149.

636 Sorokin, D.Y., K.S. Makarova, B. Abbas, M. Ferrer, P.N. Golyshin, E.A. Galinski, S. Ciordia, M.C.
637 Mena, A.Y. Merkel, Y.I. Wolf, M.C.M. van Loosdrecht, and E. V. Koonin. 2017. Discovery
638 of extremely halophilic, methyl-reducing euryarchaea provides insights into the
639 evolutionary origin of methanogenesis. Nat. Microbiol. 2(May): 17081. doi:
640 10.1038/nmicrobiol.2017.81.

641 Steinberg, L.M., and J.M. Regan. 2009. mcrA-targeted real-time quantitative PCR method to
642 examine methanogen communities. Appl. Environ. Microbiol. 75(13): 4435–4442. doi:
643 10.1128/AEM.02858-08.

644 van Teeseling, M.C.F., A. Pol, H.R. Harhangi, S. van der Zwart, M.S.M. Jetten, H.J.M. Op den
645 Camp, and L. van Niftrik. 2014. Expanding the verrucomicrobial methanotrophic world:
646 Description of three novel species of Methylacidimicrobium gen. nov. Appl. Environ.
647 Microbiol. 80(21): 6782–6791. doi: 10.1128/AEM.01838-14.

648 Thauer, R.K., A.-K. Kaster, H. Seedorf, W. Buckel, and R. Hedderich. 2008. Methanogenic
649 archaea: ecologically relevant differences in energy conservation. Nat. Rev. Microbiol.
650 6(8): 579–591. doi: 10.1038/nrmicro1931.

651 The R Core Team. 2018. R: A language and environment for statistical computing.

652 Tveit, A.T., T. Urich, P. Frenzel, and M.M. Svenning. 2015. Metabolic and trophic interactions
653 modulate methane production by Arctic peat microbiota in response to warming. Proc.
654 Natl. Acad. Sci. 112(19): E2507–E2516. doi: 10.1073/pnas.1420797112.

655 Vaksmaa, A., C. L??ke, T. van Alen, G. Val??, E. Lupotto, M.S.M. Jetten, and K.F. Ettwig.
656 2016a. Distribution and activity of the anaerobic methanotrophic community in a
657 nitrogen-fertilized Italian paddy soil. FEMS Microbiol. Ecol. 92(12): 1–11. doi:
658 10.1093/femsec-fiw181.

659 Vaksmaa, A., C. Lüke, T. van Alen, G. Valè, E. Lupotto, M.S.M. Jetten, and K.F. Ettwig. 2016b.
660 Distribution and activity of the anaerobic methanotrophic community in a nitrogen-
661 fertilized Italian paddy soil. FEMS Microbiol. Ecol. 92(12): 1–11. doi: 10.1093/femsec-
662 fiw181.

663 Walters, W., E.R. Hyde, D. Berg-lyons, G. Ackermann, G. Humphrey, A. Parada, J.A. Gilbert,
664 J.K. Jansson, J.G. Caporaso, J.A. Fuhrman, A. Apprill, and R. Knight. 2015. Improved
665 Bacterial 16S rRNA GEne(V4 and V4-V5) and Fungal Internal Transcribed Spacer Marker
666 Gene Primers for Microbial Community Surveys. mSystems 1(1): e0009-15. doi:
667 10.1128/mSystems.00009-15.Editor.

668 Welte, C.U., O. Rasigraf, A. Vaksmaa, W. Versantvoort, A. Arshad, H.J.M. Op den Camp,
669 M.S.M. Jetten, C. Lï¿½ke, and J. Reimann. 2016a. Nitrate- and nitrite-dependent
670 anaerobic oxidation of methane. Environ. Microbiol. Rep. 8(6): 941–955. doi:
671 10.1111/1758-2229.12487.

672 Welte, C.U., O. Rasigraf, A. Vaksmaa, W. Versantvoort, A. Arshad, H.J.M. Op den Camp,
673 M.S.M. Jetten, C. Lüke, and J. Reimann. 2016b. Nitrate- and nitrite-dependent
674 anaerobic oxidation of methane. Environ. Microbiol. Rep. 8(6): 941–955. doi:
675 10.1111/1758-2229.12487.

676 Wen, X., V. Unger, G. Jurasinski, F. Koebsch, F. Horn, and G. Rehder. 2018a. Predominance of
677 methanogens over methanotrophs contributes to high methane emissions in rewetted

fens. (April): 1–36.

Wen, X., V. Unger, G. Jurasinski, F. Koebsch, F. Horn, G. Rehder, T. Sachs, D. Zak, G. Lischeid, K.H. Knorr, M.E. Böttcher, M. Winkel, P.L.E. Bodelier, and S. Liebner. 2018b. Predominance of methanogens over methanotrophs in rewetted fens characterized by high methane emissions. Biogeosciences 15(21): 6519–6536. doi: 10.5194/bg-15-6519-2018.

Zalman, C.A., N. Meade, J. Chanton, J.E. Kostka, S.D. Bridgham, and J.K. Keller. 2017. Methylotrophic methanogenesis in Sphagnum-dominated peatland soils. Soil Biol. Biochem. 118(July 2017): 156–160. doi: 10.1016/j.soilbio.2017.11.025.

Ziebarth, M., U. Lenschow, and T. Permien. 2009. Konzept zum Schutz und zur Nutzung der Moore - Fortschreibung des Konzeptes zur Bestandssicherung und zur Entwicklung der Moore. : 109.